Experimental report

13/09/2019

Proposal:	**9-10-1577**	**Council:**	10/2018
Title:	Pressure-induced phase transition of micelle-forming thermoresponsivePMMA-b-PNIPAM diblock copolymers in aqueous solutions		
Research area:	Soft condensed matter		

This proposal is a continuation of 9-11-1827

Main proposer:	**Christine PAPADAKIS**
Experimental team:	Alfons SCHULTE Chia-Hsin KO Shu Hsien HUANG GEETHU PATHIRASSERY MELEDAM Leonardo CHIAPPISI
Local contacts:	Leonardo CHIAPPISI

Samples: PMMA-b-PNIPAM

Instrument	Requested days	Allocated days	From	To
D11	3	3	18/06/2019	21/06/2019

Abstract:

We wish to investigate the pressure-dependent behavior of micelle-forming PMMA-b-PNIPAM diblock copolymers in aqueous solution. Their structural changes upon crossing the coexistence line in the (p,T)-frame shall be studied by varying pressure at constant temperature. SANS at D11 will give insight into the degree of dehydration at the phase transition, which is different at low and at high pressures. Time-resolved SANS after a rapid pressure jump shall give insight into the kinetics of the phase transition (collapse and aggregation), spanning from 100 ms to few 1000 s and over a large range of length scales (~1-100 nm). These measurements extend our previous results on aqueous PNIPAM homopolymer solutions.

Pressure induced phase transition of micelle forming thermoresponsive PMMA-*b*-PNIPAM diblock copolymer in aqueous solutions

The amphiphilic diblock copolymer poly(methyl methacrylate)-*b*-poly(*N*-isopropylacrylamide) (PMMA-*b*-PNIPAM) consists of a hydrophobic PMMA block and a thermoresponsive PNIPAM block. In aqueous solution, PMMA-*b*-PNIPAM self-assembles into core-shell micelles, and the PNIPAM micellar shell collapses while heating above its cloud point [1,2]. In addition to temperature, pressure also induces a cloud point in aqueous solutions of PMMA-*b*-PNIPAM [3]. The coexistence line in the temperature-pressure phase diagram of PMMA-*b*-PNIPAM shows an elliptical shape, which offers the possibility of performing pressure-jump experiments from the one-phase state to the two-phase state, both in the low-pressure and in the high-pressure regime [4]. In the present work, we have investigated the influence of pressure on the structural changes of PMMA-*b*-PNIPAM micelles by performing time-resolved small-angle neutron scattering (SANS) experiments in combination with millisecond pressure jumps, where the collapse of the PNIPAM micellar shell and the aggregation behavior of the micelles are studied in detail.

The kinetic SANS experiments in combination with rapid pressure-jumps were performed at instrument D11 with a 50 mg/ml solution of $PMMA_{22}$-*b*-$PNIPAM_{260}$ (M_n =32000 g/mol) in D_2O. The transition temperatures of the solution were precisely located by performing temperature scans from 25°C to 35°C at three different pressures, namely 0.1 MPa, 35 MPa and 75 MPa. Before performing each pressure jump, the samples were equilibrated in the one-phase region for 30 min to eliminate possible hysteresis effects. Further, the following pressure-jump experiments were performed across the co-existence line as well as within the one-phase state in order to understand the effect of pressure on the collapse of PNIPAM shell and the aggregation behavior of the collapsed micelles.

1. $T = 32.1°C$; $P_i = 35$ MPa, $P_f = 10$ MPa, $\Delta P = 25$ MPa
2. $T = 31.8°C$; $P_i = 35$ MPa, $P_f = 10$ MPa, $\Delta P = 25$ MPa
3. $T = 31.8°C$; $P_i = 60$ MPa, $P_f = 85$ MPa, $\Delta P = 25$ MPa
4. $T = 31.8°C$; $P_i = 60$ MPa, $P_f = 100$ MPa, $\Delta P = 40$ MPa

where P_i, P_f and ΔP respectively represent the initial pressure, final pressure and the magnitude of the pressure jump. After each pressure jump, 95 frames, each having an exposure time of 0.05×1.1^n s (where $n = 1, 2, 3,\ldots 95$), were captured. A combination of three sample-to-detector distances (SDD = 1.5 m, 8 m and 34 m) at a mean wavelength $\lambda = 6$ Å with a wavelength resolution $\Delta\lambda/\lambda$ of ∼10% were used to cover a scattering vector range of q = 0.002-0.3 $Å^{-1}$ [$q = 4\pi \sin(\theta/2)/\lambda$, where θ is the scattering angle]. The measurements at SDD = 34m were repeated 4 times for better statistics. The sample was mounted in a copper beryllium cell (21 PL 30 A 02) of thickness 2 mm, which is capable of withstanding pressures up to 350 MPa. The measured data were corrected for background and empty cell contributions and normalized to absolute cross sectional units using standard procedures. Data reductions were performed using the LAMP software.

SANS profiles together with the fitted models for temperature scans performed at 0.1 MPa, 35 MPa and 75 MPa are shown in Figure 1 (a-c), respectively. With increasing temperature, the scattered intensity in the low q regime increases strongly indicating the formation of larger aggregates from micelles with collapsed shells.

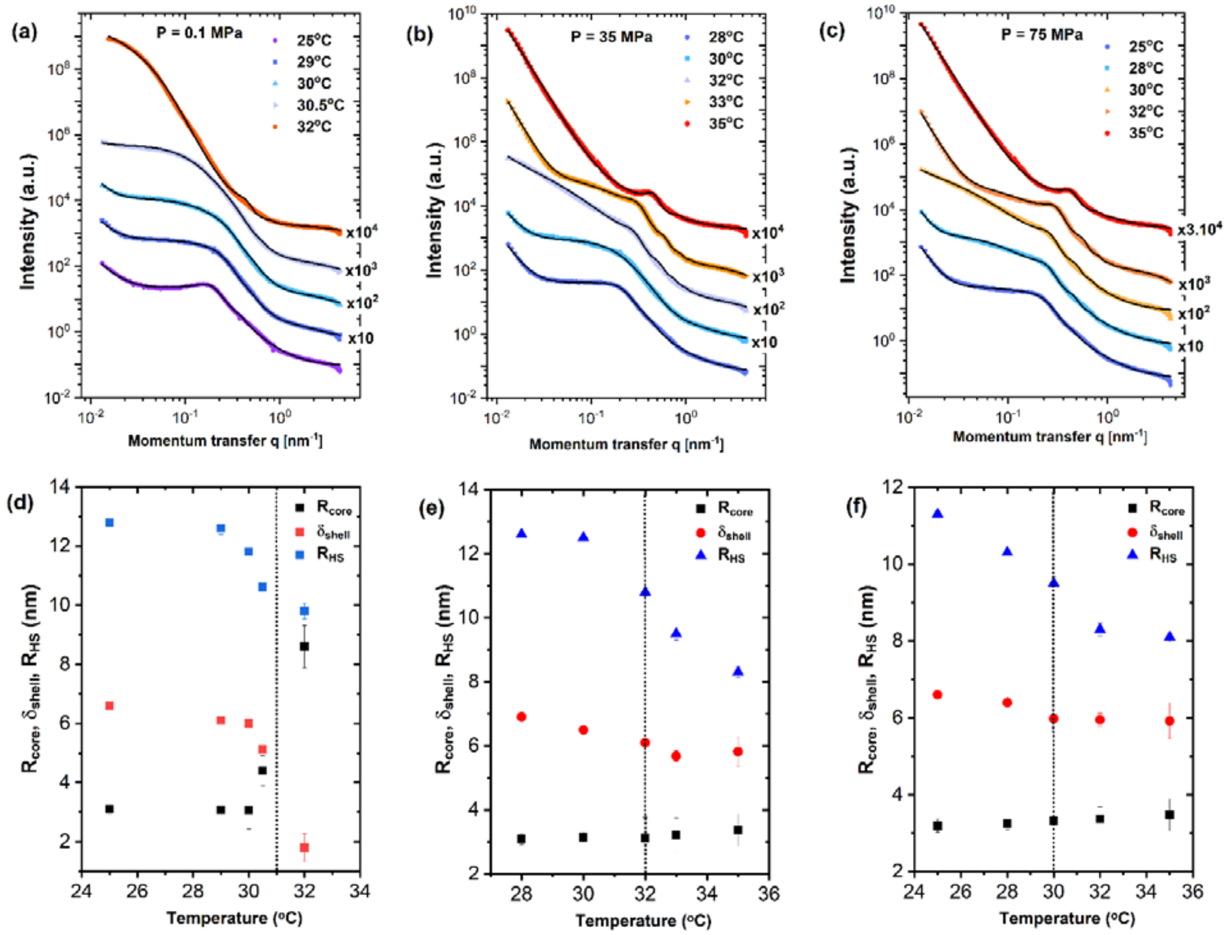

Figure 1: (a-c) SANS profiles together with best fits for temperature scans in the range from 25°C up to 35°C for a 50 mg/ml PMMA-*b*-PNIPAM solution at 3 different pressures: (a) 0.1 MPa, (b) 35 MPa and (c) 75 MPa. The curves are shifted as indicated. (d-f) Core radius, shell thickness and hard-sphere radius obtained from the best fits to the SANS profiles at (d) 0.1 MPa, (e) 35 MPa and (f) 75 MPa. The dotted vertical lines indicate the cloud points.

The scattering curves are fitted with the following function [2].

$$I(q) = P_{mic}(q)S_{SHS}(q) + S_{OZ}(q) + I_{agg}(q) + I_{bkg} \qquad (1)$$

Here, $P_{mic}(q)$ is the form factor for spherical core-shell micelles, $S_{SHS}(q)$ the sticky hard sphere structure factor which represents the intermicellar interactions, $S_{OZ}(q)$ the Ornstein–Zernike term for the thermal fluctuations. $I_{agg}(q)$ corresponds to the scattering from micellar aggregates which is parametrized by the Porod form factor and I_{bkg} represents the incoherent scattering background. The variation of core radius, shell thickness and the hard-sphere radius of PMMA-*b*-PNIPAM micelles with temperature, at the three pressures, obtained from the best fits of the SANS profiles are portrayed in Figure 1 (d-f). As shown in Figure 1 (d), at 0.1 MPa, an increase in core radius and a considerable decrease in shell thickness are noted above the cloud point. These observations are attributed to the strong dehydration and the subsequent collapse of the PNIPAM shell. In contrast, at 35 MPa and 75 MPa, the core radius and shell thickness do not show any significant changes, indicating that the PNIPAM shell stays hydrated even above the cloud point. Further, at all pressures, the hard-sphere radius decreases while approaching the cloud point owing to the increase in inter-micellar interactions. From the temperature scans, it is evident that the transition from the one-phase state to the two-phase state can be identified as the temperature at which the scattered intensity in the low q regime shows a significant increase indicating the formation of larger micellar aggregates.

Figure 2 (a) shows exemplarily the SANS profiles after the pressure jump $\Delta P = 25$ MPa in the low pressure regime ($P_i = 35$ MPa, $P_f = 10$ MPa) performed at a constant temperature of 32.1°C. The shoulder at around 0.3 nm^{-1} shifts to lower q values over time, which indicates the increase in size of the hydrophobic scattering core of the micelles. This can be attributed to the contribution from the dehydrated PNIPAM shell towards scattering together with the hydrophobic PMMA core. Further, the intensity of forward scattering increases with time which implies the formation of larger micellar aggregates driven by the hydrophobic interactions. The variation of the size of hydrophobic entities of micelles (core radius) as a function of time obtained by best fitting Eq. 1 to the SANS profiles is shown in Figure 2 (b). The gradual increase in core radius with time implies that the collapse of PNIPAM shell is rather gradual in contrast to the rapid water expulsion and mesoglobule formation in PNIPAM homopolymer solutions [4]. In fact, we noticed a shallower elliptical shape of the coexistence line in the temperature-pressure frame for PMMA-*b*-PNIPAM in comparison to the more pronounced elliptical phase diagram of PNIPAM homopolymer, which supports this observation.

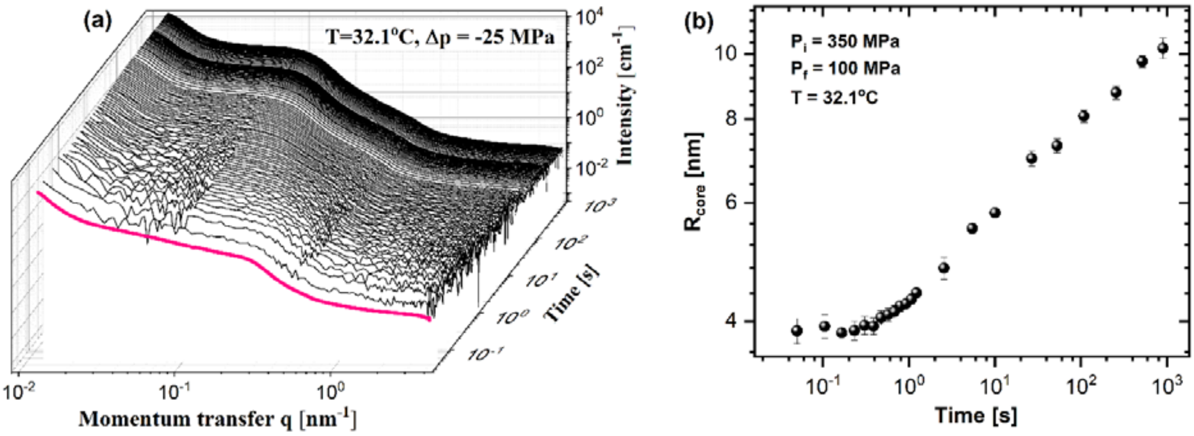

Figure 2: (a) SANS profiles of the 50 mg/ml PMMA-*b*-PNIPAM solution in D_2O after the pressure jump with $P_i = 35$ MPa, $P_f = 10$ MPa, and $\Delta P = 25$ MPa at 32.1°C. The pink curve shows the prerelease measurement. (b) Core radius of the micelles as a function of time obtained from the best fits of Eq. 1 to the scattering curves shown in (a).

Further analysis of the scattering profiles and the interpretation of results will give insights regarding the growth process of micellar aggregates and the role of the degree of dehydration of PNIPAM shell in governing the growth process.

The experiment was very successful. We thank Dr. Leonardo Chiappisi and Dr. Ralf Schweins for the excellent support during the beam time.

[1] J. Adelsberger, C. M. Papadakis et al., Macromol. Rapid Commun. **2012**, 33**,** 254−259.
[2] J. Adelsberger, C. M. Papadakis et al., *Soft Matter* **2013**, *9*, 1685.
[3] B.-J. Niebuur, C.M. Papadakis et al., *ACS Macro Lett.* **2017**, *6*, 1180.
[4] B.-J. Niebuur, C.M. Papadakis, et al. *ACS Macro Lett.* **2018**, *7*, 1155.